Long-range effects on superdiffusive algebraic solitons in anharmonic chains

C. Brunhuber[1,a], F.G. Mertens[1], and Y. Gaididei[2]

[1] Physikalisches Institut, Universität Bayreuth, Germany
[2] Bogolyubov Institute for Theoretical Physics, 03143 Kiev, Ukraine

Abstract. Studies on thermal diffusion of lattice solitons in Fermi-Pasta-Ulam (FPU)-like lattices were recently generalized to the case of dispersive long-range interactions (LRI) of the Kac-Baker form. The variance of the soliton position shows a stronger than linear time-dependence (superdiffusion) as found earlier for lattice solitons on FPU chains with nearest-neighbour interactions (NNI). Since the superdiffusion seems to be generic for nontopological solitons, we want to illuminate the role of the soliton shape on the superdiffusive mechanism. Therefore, we concentrate on an FPU-like lattice with a certain class of power-law long-range interactions where the solitons have algebraic tails instead of the exponential tails in the case of FPU-type interactions (with or without Kac-Baker LRI). Despite of structurally similar Langevin equations which hold for the soliton position and width of the two soliton types, the algebraic solitons reach the superdiffusive long-time limit with a characteristic $t^{3/2}$ time-dependence much faster than exponential solitons. The soliton shape determines the diffusion constant in the long-time limit that is approximately a factor of π smaller for algebraic solitons. Our results appear to be *generic* for nonlinear excitaitons in FPU-chains, because the same superdiffusive time-dependence was also observed in simulations with discrete breathers.

PACS. 05.10.Gg Stochastic analysis methods (Fokker-Planck, Langevin, etc.) – 05.45.Yv Solitons – 05.40.-a Fluctuation phenomena, random processes, noise, and Brownian motion – 05.50.+q Lattice theory and statistics (Ising, Potts, etc.)

1 Introduction

Nonlinear excitations like solitons and discrete breathers have been drawing great attention over recent years. They present very robust solutions of nonlinear partial differential equations and nonlinear lattice models which are often used to describe a rather broad set of physical systems [1–3]. Nonlinear lattices like Klein-Gordon (KG), Fermi-Pasta-Ulam or the discrete nonlinear Schroedinger (DNLS) lattice (and their counterparts in the continuum approximation) present all to often a strong approximation of the system of interest and it is sometimes not clear to what extend solitons or discrete breathers are also relevant in more realistic models. In the case of biomolecules, the aspiration to highlight their basic functionalities with computer simulations is a challenging task for the computational science nowadays. If we aim to understand principally the role of nonlinear excitations in biomolecules, we have to investigate simpler models than the numerical ab initio calculations. Often used in this context is

ᵃ e-mail: btp342@uni-bayreuth.de

the Davydov model [4,5] for energy and charge transport in proteins or the Peyrard-Bishop-Dauxois (PBD) model which describes the melting and the denaturation of DNA [6,7]. There are convincing evidences that some features of nonlinear excitations in this simplified models are relevant in explaining the functionality of biomolecules. Recently, pump-probe measurements [8] showed that the lifetime of NH stretching bands in the model protein ACN is (with about 18 ps) in good agreement with numerical calculations of the Davydov model [9]. The observation that the PBD model succeeds in determining the thermally induced openings of the DNA strand at functionally relevant sites for the DNA transcription [10] is also an example for the relevance of nonlinear lattice models in biology.

Nowadays, many physicists who work in this field try to extend and improve the basic models in order to make them more realistic. The spatial structure of biomolecules, thermal fluctuations, damping and long-range effects stemming from Coulomb or dipole-dipole interactions have certainly a great influence on the nonlinear excitations and the statistics of the system. It is known that long-range effects can change the features of solitons

and discrete breathers qualitatively when the LRI exceed some critical value [11,12]. In FPU-like chains and nonlinear Schrödinger models, they give rise to new types of solitons which can coexist at the same value of the spectral parameter [13]. Controlled switching between such soliton states was recognized as a possible mechanism for energy transport and storage in biomolecules [14]. In the past, nonlinear KG lattices with LRI were frequently studied in investigations of a number of physical phenomena such as dislocations in solids, charge density waves, absorbed layers of atoms or domain walls in ferromagnets and ferroelectrics (see references in [15–17]). The effect of thermal fluctuations and LRI are usually regarded separately [9,18,19] because of their complexity. Nevertheless it is known that LRI can have very interesting effects on the thermodynamics of many different physical systems [20,21].

The Kac-Baker form presents a spatially exponential coupling between different particles which is quite often chosen for the inclusion of LRI in nonlinear lattice models [11,21,22]. In the recent publication [23] lattice solitons on FPU-like chain with Kac-Baker LRI in the presence of a thermal reservoir were investigated. In the continuum approximation of the system and with a collective variable (CV) approach, it was possible to derive a Langevin set of equations for the soliton position, similar to the solitons on FPU chains [24]. The solitons on FPU chains (with or without Kac-Baker LRI) show superdiffusive behaviour. The position variance of the soliton shows, besides the linear term in the time-dependence, also quadratic and cubic terms. In [23], it was demonstrated, that the diffusion mechanism for NNI and for additional LRI are quite similar because the same CV ansatz was used. In the case of Kac-Baker LRI, this approximation is valid unless the soliton velocities do not reach the critical velocity, where the soliton begins to develop a cusp [11].

Superdiffusion of nonlinear excitations in FPU-chains was also observed in simulations, where a high-amplitude localized excitation was injected in the center of a thermalized FPU-chain, and a mean-square displacement $\sim t^{3/2}$ was obtained for different force constants and temperatures [25]. Interestingly, the diffusion of the localized excitations seems to stem here from the scattering with low-energy breathers, the possibility of a fluctuating breather shape was not discussed.

In order to check the influence of the soliton shape on the diffusion of the soliton, we choose a power-law coupling. This leads in the continuum approximation (CA) to a Benjamin-Ono (BO) equation, which is known to posses algebraic soliton solutions [26]. The first studies in that direction date back to Ishimori [28] who studied anharmonic chains with Lennard-Jones $(2n, n)$ intermolecular potential and showed that the dynamics is governed by the Benjamin-Ono equation in the case $n = 2$ or by the Korteweg-de Vries equation for $n \geq 4$. In the case of cubic and quartic nearest-neighbour interactions, a reductive perturbation method yields a $KdV + mKdV$ and Benjamin-Ono equation which was shown to possess exact nonsingular rational solutions [27].

2 The model

Our model is a one-dimensional chain of equally spaced particles of mass m ($m = 1$) with an interatomic spacing a ($a = 1$). We denote the displacement of the particle n from its equilibrium position as u_n (absolute displacement coordinates) and the difference $w_n = u_{n+1} - u_n$ as relative displacement coordinates. The potential consists of a part U_{NN} similar to the original potential chosen by Fermi, Pasta and Ulam and a long-range potential U_{LR} with a power-law dependence of the harmonic coupling constant J_{nm}

$$T = \frac{1}{2} \sum_{n=1}^{N} \left(\frac{du_n(t)}{dt} \right)^2 \qquad (1)$$

$$U_{NN} = \sum_{n=1}^{N} V(u_{n+1}(t) - u_n(t)) \qquad (2)$$

$$V(r) = \frac{r^2}{2} - \frac{r^3}{3} \qquad (3)$$

$$U_{LR} = \frac{1}{2} \sum_{n} \sum_{m \neq n} \frac{J}{|m - n|^s} (u_n - u_m)^2. \qquad (4)$$

The model covers the physical situation of dipole-dipole ($s = 5$) and Coulomb interactions ($s = 3$) between the particles on the chain, if we restrict ourselves to small relative displacements. The equation of motions in relative displacement coordinates can be obtained from the Lagrangian of the system $L = T - U_{NN} - U_{LR}$

$$\ddot{w}_i(t) = V'(w_{i+1}) - 2V'(w_i) + V'(w_{i-1})$$
$$- J \sum_{m \neq 0} \frac{(w_i - w_{i+m})}{|m|^s}. \qquad (5)$$

When we want to consider the effect of a thermal bath, we can add damping and white noise terms to the original equation (5) such that they fulfill the fluctuation-dissipation theorem ($D^{hy} = 2\nu_{hy}T$ with k_B set to unity) [24]

$$\ddot{w}_i(t) = V'(w_{i+1}) - 2V'(w_i) + V'(w_{i-1})$$
$$- J \sum_{m \neq 0} \frac{(w_i - w_{i+m})}{|m|^s} + \nu_{hy}(\dot{w}_{i+1} - 2\dot{w}_i + \dot{w}_{i-1})$$
$$+ \sqrt{D^{hy}}(\xi_{i+1}(t) - \xi_i) = 0 \quad (6)$$

$$\langle \xi_i(t)\xi_j(s) \rangle = \delta(t - s)\delta_{ij}. \qquad (7)$$

We choose hydrodynamical damping which depends on the relative displacement velocities of the particles and presents an intrinsic damping mechanism of the system. The widely used Stokes damping is not appropriate for pulse solitons because one obtains an imaginary dispersion relation the long-wave region of the Fourier spectrum what causes deformations of the soliton [29]. We go to the continuum limit [$w_i(t) \to w(x,t)$, $\xi_i(t) \to \xi(x,t)$,

$f(x+m,t) \rightarrow e^{m\partial_x}f(x,t)]$ and find the partial differential equation (PDE)

$$
\partial_t^2 w(x,t) = 2(\cosh(\partial_x) - 1)V'(w(x,t))
$$
$$
- 2J \sum_{m=1}^{\infty} \frac{1 - \cosh(m\partial_x)}{m^s} w(x,t) + \nu_{hy}\partial_x^2\partial_t w(x,t)
$$
$$
+ \sqrt{D^{hy}}\partial_x^2\xi(x,t). \quad (8)
$$

The further treatment of the system depends on the value of s. In [26] it is shown that in the case $s > 5$ the CA yields a Boussinesq equation similar to the result without LRI but with a different dispersion parameter. For $3 < s \leq 5$ it was proved that the soliton tails are no longer exponential but algebraic and that for $s \leq 3.5$ an energy gap between the soliton states and the plane wave spectra appears. For $s = 4$, the equation of motion becomes a Hilbert-Boussinesq equation which can be reduced to the integrable Benjamin-Ono form, which has algebraic soliton solutions.

Since the soliton equation in [23] was of Boussinesq-type and covered the limit of nearest-neighbour interactions, we do not expect fundamental new effects for $s > 5$. The choice $s = 5$ and $s = 3$ represent physically interesting situations since this corresponds to Coulomb ($s = 3$) and dipole-dipole ($s = 5$) interactions. Instead of investigating this two situations, we choose the intermediate case $s = 4$ to investigate the behaviour of solitons with algebraic tails. Opposite to the physically relevant cases $s = 3$ and $s = 5$, our choice $s = 4$ leads to an analytically easier to handle model, a Hilbert-Boussinesq equation with the resulting Benjamin-Ono-type soliton solutions. The perturbed Hilbert-Boussinesq equation

$$
\partial_t^2 w - c^2\partial_x^2 w - \lambda\partial_x^4 w - \frac{J\pi}{6}\mathcal{H}(\partial_x^3 w) + 2\partial_x^2 w^2 =
$$
$$
\nu_{hy}\partial_x^2\partial_t w + \sqrt{D^{hy}}\partial_x\xi(x,t) \quad (9)
$$

with $c^2 = (1 + J\pi^2/6)$ und $\lambda = (1/12 - J/24)$ follows from expanding in (8) the operators for the nearest-neighbour part and for the long-range part $Q(s,\partial_x) = 2\sum_m (1 - \cosh(m\partial_x))/m^s$

$$
2(\cosh(\partial_x) - 1) = 2\left(\frac{\partial_x^2}{2!} + \frac{\partial_x^4}{4!} + ...\right) \quad (10)
$$

$$
Q(4,\partial_x) = -\frac{\pi^2}{6}\partial_x^2 - \frac{\pi}{6}\mathcal{H}(\partial_x^3) + \frac{1}{24}\partial_x^4, \quad (11)
$$

where $\mathcal{H}(f(x)) = 1/\pi P \int_{-\infty}^{\infty} f(y)/(y-x)dy$ denotes the Hilbert transform and P the Cauchy principal value. Similarly like in [23], we will have to rewrite the soliton equation (9) in absolute displacement coordinates in order to find its Lagrangian density (in the case $\nu_{hy} = 0$). Notice that the λ-term was neglected in reference [26].

3 Collective variables

The Hilbert-Boussinesq equation in absolute displacement coordinates $u(x,t)$ ($w = \partial_x u$)

$$
\partial_t^2 u - c^2\partial_x^2 u - \lambda\partial_x^4 u - \frac{J\pi}{6}\mathcal{H}(\partial_x^3 u) + 2\partial_x u\partial_{xx} u =
$$
$$
\nu_{hy}\partial_x^2\partial_t u + \sqrt{D^{hy}}\partial_x\xi(x,t) \quad (12)
$$

can be derived for $\nu^{hy} = 0$ from the Lagrangian density

$$
\mathcal{L} = \frac{u_t^2}{2} - \frac{c^2 u_x^2}{2} + \frac{u_x^3}{J\pi} + \frac{J\pi}{6}u_{xx}\mathcal{H}(u_x) + \lambda\frac{u_{xx}^2}{2}
$$
$$
- \sqrt{D^{hy}}u_x\xi(x,t). \quad (13)
$$

As a CV ansatz with $X(t)$ and $\sigma(t)$, we will use the Benjamin-Ono-type soliton shape

$$
u(x,t) = -A_o\text{Arctan}[\sigma(t)(x - X(t))]. \quad (14)
$$

One can check that this ansatz yields the correct values

$$
A_o = \frac{J\pi}{3} + 4\lambda\sigma_o, \ \sigma_o = \frac{6}{\pi J}(v^2 - c^2) \quad (15)
$$

(compare with [14]) when one minimizes the action for

$$
\langle\mathcal{L}\rangle = \int_{-\infty}^{+\infty} dx\mathcal{L} = \frac{A_o^2\pi}{4}\left(\frac{\dot{\sigma}^2}{\sigma^3} + \sigma\dot{X}^2\right)
$$
$$
- \frac{c^2 A_o^2\pi\sigma}{4} - \frac{\pi}{8}A_o^3\sigma^2 + \frac{A_o^2 J\pi^2\sigma^2}{48} + \frac{A_o^2\pi\gamma\sigma^3}{8}
$$
$$
+ \sqrt{D^{hy}}\int_{-\infty}^{+\infty} dx\frac{A_o\sigma}{1 + \sigma^2(x - X(t))^2}\xi(x,t). \quad (16)
$$

(with $\lambda = 0$ and $\sqrt{D^{hy}} = 0$) for the soliton parameters σ, A_o and $X(t)$ assuming a coherent excitation with constant velocity ($\dot{\sigma} = \dot{A}_o = 0$, $\dot{X} = v$).
To include the damping, we proceed like in [23] with the generalized Hamilton principle of Ostrovsky et al. [30,31]

$$
\frac{\delta\langle\mathcal{L}\rangle}{\delta X_i} = \frac{\partial\langle\mathcal{L}\rangle}{\partial X_i} - \frac{\partial}{\partial t}\frac{\partial\langle\mathcal{L}\rangle}{\partial\dot{X}_i} = -\langle\Phi u_i\rangle, \quad (17)
$$

where $\Phi = \nu_{hy}u_{xxt}$ is a dissipative field and the brackets signify a spatial integration over x.

In Figure 1, we show two solitons with $c_o = v/c = 1.01$ (left panel) and $c_o = 1.03$ (right panel) on FPU chains with power-law LRI ($s = 4$, $J = 0.7877$, $c = 1.51516$) and for the Kac-Baker LRI (described in [23]). The values of α and J for the solitons with the exponential tails in the Kac-Baker case were chosen to produce a solution with the same velocity and soliton energy H. The power-law LRI yield solutions with Lorentzian shape (algebraic solitons) whereas the Kac-Baker LRI yield solitons which are well approximated by a *sech* (exponential solitons).
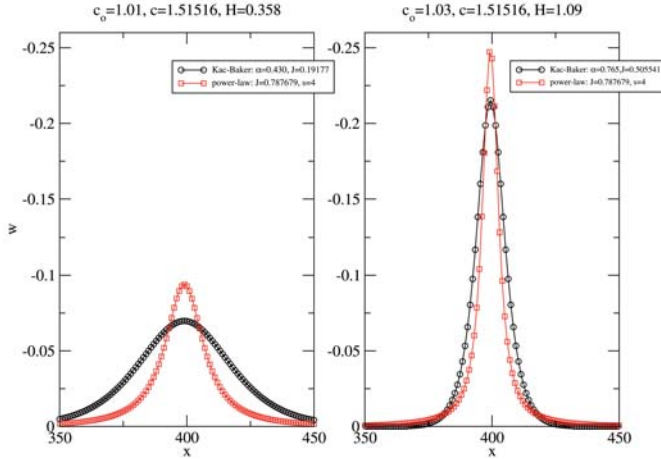
Fig. 1. (Color online) Soliton solutions for power-law ($s = 4$) and Kac-Baker long-range interactions. The two solitons in the left and the right panel each have the same velocity $c_o = v/c$ (v: soliton velocity) and the same energy H.

4 Langevin system

Equations (17) together with the ansatz (14) leads to following stochastic equations for the collective variables $\sigma(t)$ and $X(t)$:

$$\dot{\sigma}\dot{X} = \frac{4\sqrt{D^{hy}}\sigma^3}{A_o\pi}\int_{-\infty}^{+\infty}dx\frac{\bar{x}\xi(x,t)}{(1+\sigma^2\bar{x}^2)^2} - \frac{\nu_{hy}}{2}\dot{X}\sigma^3 \tag{18}$$

$$(\dot{X}^2 - c^2) = \frac{A_o\sigma}{2} + \frac{\lambda\sigma^2}{2} - \frac{8\sqrt{D^{hy}}\sigma^2}{\pi A_o}\int_{-\infty}^{+\infty}dx\frac{\bar{x}^2\xi(x,t)}{(1+\sigma^2\bar{x}^2)^2} \tag{19}$$

with

$$A_o = \frac{J\pi}{3} + 4\lambda\sigma_0, \quad \bar{x} = x - X(t). \tag{20}$$

In the previous step, we neglected small terms $\sim\dot{\sigma}^2$, $\sim\ddot{X}$ and $\ddot{\sigma}$ in order to obtain technically less comprehensive stochastic equations. The justification of this step was checked by numerical simulations of the complete system and was already successfully applied in the case of Kac-Baker LRI [23].

Like in [23], we rewrite the equation (19) as an equation for $\dot{X}$

$$\dot{X}^2 = v_d^2\left(1 - \frac{1}{v_d^2}\frac{8\sqrt{D^{hy}}\sigma^2}{\pi A_o}\int_{-\infty}^{+\infty}dx\frac{\bar{x}^2\xi(x,t)}{(1+\sigma^2\bar{x}^2)^2}\right). \tag{21}$$

We expand the appearing square root for the small parameter $\sqrt{D^{hy}}$ to first order and approximate the velocity

$$v_d = \sqrt{c^2 + \frac{A_o}{2}\sigma(t) + \frac{\lambda}{2}\sigma(t)^2} \tag{22}$$

in the stochastic term with the start velocity v of the soliton (because $c < v_d < v$, $c \sim v$). We end up in a

system of stochastic integro-differential equations for the CV:

$$\begin{pmatrix}\dot{\sigma}\\\dot{X}\end{pmatrix} = \begin{pmatrix}A_1\\A_2\end{pmatrix} + \int_{-\infty}^{+\infty}dx\begin{pmatrix}B_{11} & 0\\0 & B_{22}\end{pmatrix}\begin{pmatrix}\xi\\\xi\end{pmatrix}, \tag{23}$$

with

$$A_1 = -\frac{\nu_{hy}}{2}\sigma^3, \quad A_2 = v_d \tag{24}$$

$$B_{11} = \frac{4\sqrt{D^{hy}}\sigma^3}{\pi A_0 v}\frac{(x - X(t))}{(1 + \sigma^2(x - X(t))^2)^2} \tag{25}$$

$$B_{22} = -\frac{4\sqrt{D^{hy}}\sigma^2}{\pi A_0 v}\frac{(x - X(t))^2}{(1 + \sigma^2(x - X(t))^2)^2}. \tag{26}$$

We proceed like in [24,32] in order to find a statistically equivalent Langevin system to (23) (with the same Fokker-Planck equation in the Stratonovich interpretation [33]) which is more convenient for further numerical and analytical studies. The Langevin-system with two independent Gaussian white noise processes reads:

$$\begin{pmatrix}\dot{\sigma}\\\dot{X}\end{pmatrix} = \begin{pmatrix}a_1\\a_2\end{pmatrix} + \begin{pmatrix}b_{11} & 0\\0 & b_{22}\end{pmatrix}\begin{pmatrix}\xi^1\\\xi^2\end{pmatrix} \tag{27}$$

with

$$a_1 = -\frac{\nu_{hy}\sigma^3}{2} - \frac{D^{hy}\sigma^2}{4A_o^2\pi v^2}, \quad a_2 = v_d$$

$$b_{11} = \frac{\sqrt{D^{hy}}\sigma^{\frac{3}{2}}}{A_o\sqrt{\pi}v}, \quad b_{22} = \frac{\sqrt{D^{hy}}}{\sqrt{\sigma}A_o\sqrt{\pi}v}. \tag{28}$$

The corresponding system in [23] depends similarly on the soliton parameters inverse width, A_o, velocity v and on the temperature. Only numerical constants and the velocity v_d are different. The broadening of the soliton due to the damping follows the same manner as for exponential solitons in [24,23]. The result (27) manifests the statement made in [23], that the LRI and the resulting soliton shape determine the velocity $v_d(\sigma(t))$ of the damped soliton.

5 Small-noise expansion

We proceed with a small-noise expansion for the parameter $\sqrt{D^{hy}}$ like in [23,24] in order to derive an analytical expression for the soliton diffusion. The Langevin system (27) is formally very similar to the sytem in [23] for Kac-Baker LRI, only numerical constants and the soliton parameters are different. For algebraic solitons, we can approximate (22) with $v_d = c + A_o/4c\,\sigma(t)$ because of the smallness of $\lambda = 1/12 - J/24 < A_o \sim 1$ for the solitons in Figure 1. The analytical solution in this case is technically less extensive and leads practically to the same results. The approximation for v_d is not possible in the case of Kac-Baker LRI in [23] because the long-range forces yield a larger term which is quadratic in the inverse soliton width.

The result in the first order of $\sqrt{D^{hy}}$ reads (see Appendix)

$$\mathrm{Var}[X(t)] = D^{hy} \bigg(\frac{-16A_o^2(-1+\sqrt{\eta})}{60A_o^2c^2\nu_{hy}^3\pi\sigma_o^3v^2\eta^{\frac{3}{2}}}$$

$$+\frac{A_o^2(\eta-1)(18-10\sqrt{\eta}+(\eta-1)(\eta+2))}{60A_o^2c^2\nu_{hy}^3\pi\sigma_o^3v^2\eta^{\frac{3}{2}}}$$

$$-\frac{2c^2\nu_{hy}^2\eta(-1+\sqrt{\eta}-(\eta-1)(\eta+1))}{3A_o^2c^2\nu_{hy}^3\pi\sigma_o^3v^2\eta^{\frac{3}{2}}}\bigg) \qquad (29)$$

with

$$\eta = 1 + t_r = 1 + \sigma_o^2\nu_{hy}t. \qquad (30)$$

The time-dependence of the position variance depends on the time scale t_r, which explains that the large time limit (and the superdiffusive behaviour) sets in earlier for high-velocity solitons (large values of σ_o) for the same damping constant. The corresponding result for Kac-Baker LRI is even more complex, which stems from the longer expression for v_d [23]. The time scale which describes the broadening of the exponential soliton and the diffusion is $t_r = 1.6\nu_{hy}\gamma_o^2t$ where $\gamma(t)$ is the inverse width of the exponential soliton (see [23])

We are interested in the soliton diffusion for large times t_r. Substituting (30) into (29) and looking for the leading order of t_r yields:

$$\mathrm{Var}[X(t)]_{inf} \approx \frac{D^{hy}}{60c^2\nu_{hy}^{1.5}\pi v^2}t^{1.5}, \qquad (31)$$

which differs from the result in [23] only by the numerical constant. For very small times, the result (29) gives a linear time-dependence

$$\mathrm{Var}[X(t)]_0 = \frac{4}{3}\frac{D^{hy}}{A_o^2\pi\sigma_o^2v^2}t. \qquad (32)$$

The results of the small-noise expansion shows the same characteristic dependencies on the soliton parameters as for Kac-Baker LRI in [23]. For intermediate times, the result (29) describes the transition when the position variance turns from the small-time dependence into the long-time limit wherefore a stronger increase in time (mainly $\sim t^2$) can be observed.

6 Simulations

The simulation of system (6) was performed in the same manner as described in [23] but with power-law long-range coupling instead of the Kac-Baker LRI. The position variance of the soliton was calculated from 100 different realizations of the chain. We used the solitons depicted in Figure 1 as initial conditions of the chain. The soliton with $c_o = 1.01$ ($\sigma_o \approx 0.1$) is much broader than the lattice spacing whereas the soliton with $c_o = 1.03$ ($\sigma_o \approx 0.3$) is rather discrete in the soliton center. The coupling parameter is always fixed at the value $J = 0.7877$ which yields
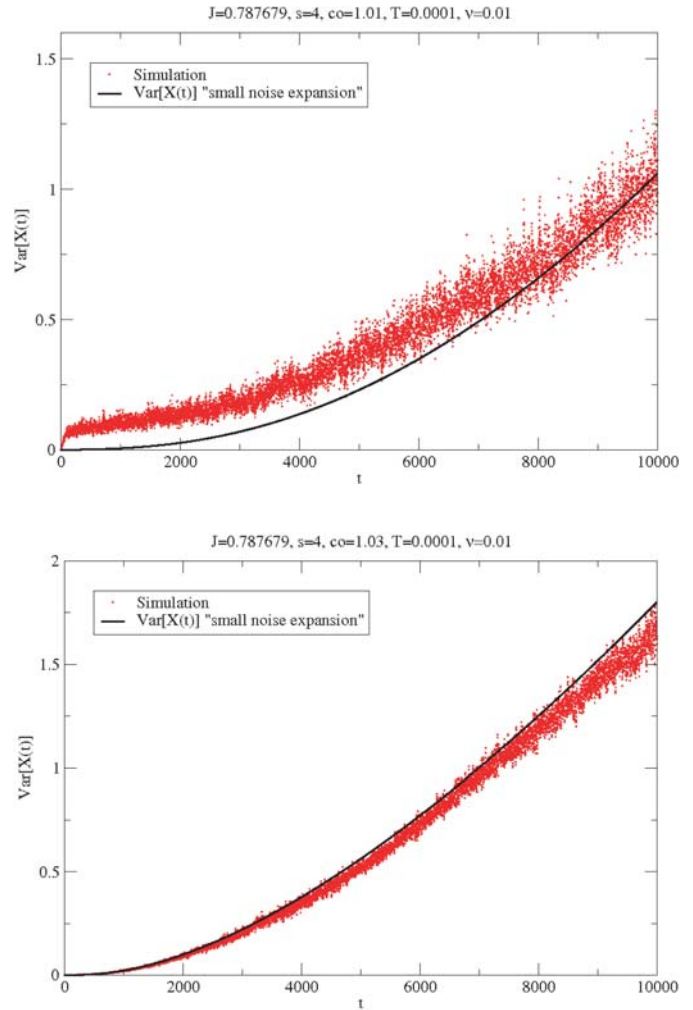

Fig. 2. (Color online) Position variance of a low-velocity (1.01) and a high-velocity (1.03) soliton on a anharmonic chain with power-law long-range interactions ($J = 0.7877$, $s = 4$). We compare the simulation results with equation (29), the result of a small-noise expansion of the Langevin system (27) of the CV theory.

the sound velocity $c = 1.51516$, the same value was used in [23]. In order to compare the results of the Kac-Baker LRI with the power-law LRI and to be able to draw meaningful conclusions , we also use the same damping constant $\nu_{hy} = 0.01$ and the same temperature $T = 0.0001$ as in reference [23].

The analytical result for the position variance (29) agrees rather well with the simulation results (Fig. 2). In general, one expects the analytical results to be slightly smaller than the simulation results because the possible contribution of phonons is not regarded in the calculations of Section 3. It was shown for a related short-range model that the phonons have indeed a perceptible influence on the soliton diffusion [35]. The analytical result for the low-velocity soliton diffusion for $c_o = 1.01$ is too small for small times. Similar discrepancies appeared for Kac-Baker LRI in [23] and they were interpreted as the

influence of phonons which cause higher values in the simulations. The analytical result for the high-velocity soliton $c_o = 1.03$ deviates from the simulation results for large times. This feature seems to stem from our restriction to first order perturbations in the small-noise expansion. When the solitons are very narrow, the width of the soliton changes quite fast and the first-order correction of $\sigma(t)$ can fail. Such deviations were also observed for FPU chains with or without Kac-Baker LRI [23,36].

The analytical result for the soliton diffusion depends only on the time scale $t_r = \nu_{hy}\sigma_o^2 t$ and for large times the diffusion should approach the result (31) from below. Since the time scale t_r depends on the width of the soliton, the long-time approximation for the position variance for high-velocity solitons will be valid for smaller values of t than for low-velocity solitons. For $c_o = 1.03$ ($\sigma_o \approx 0.3$) $t_r > 1$ is valid for $t > 1111$ whereas the corresponding time for $c_o = 1.01$ ($\sigma_o \approx 0.1$) is $t > 10\,000$. Therefore, we will check the validity of the long-time approximation result of the position variance for the soliton with $c_o = 1.03$. In deriving the long-time limit (31) of the position variance, we recognized that the approximation

$$\mathrm{Var}[X(t)]_h \approx \frac{D^{hy}}{60c^2\nu_{hy}^2\pi\sigma_o^3 v^2} \frac{t_r^3}{t_r^{1.5} + 1.5\sqrt{t_r}} \qquad (33)$$

describes the simulation results very well for all times t. Neglecting the $\sqrt{t_r}$-term for large t_r yields immediately the result (31).

The comparison between the simulation results and $\mathrm{Var}[X(t)]_h$ or $\mathrm{Var}[X(t)]_{inf}$ in Figure 3 shows that there is practically no linear dependence on t similarly as for high-energy solitons with exponential tails with Kac-Baker LRI in [23]. The superdiffusion with stronger-than-linear terms in the time-dependence of the position variance is the dominating mechanism for high-energy solitons. The time-dependence of $\mathrm{Var}[X(t)]_h$ describes the simulation results very well for all times and the soliton can be described by a time-dependence according to (31) ($\sim t^{3/2}$) for large times. For lower soliton energies like for $c_o = 1.01$ (Fig. 2) the normal contributions on $\mathrm{Var}[X(t)]$ are stronger and a comparison with $\mathrm{Var}[X(t)]_{inf}$ yields a worse agreement because in this case the limit of large t_r can not be used for $t < 10\,000$.

In the limit of short times ($t_r \ll 1$), the quality of the result for the linear contribution in time (32) is very similar to the Kac-Baker case and yields values for $\mathrm{Var}[X(t)]$ which are smaller than the simulation results. For the soliton with $c_o = 1.01$ the slope of (32) is approximately half of the value one would get from a linear fit of the simulation results for small times.

7 Comparison

Up to now, we have mentioned the similarities between the thermal diffusion of solitons with algebraic and exponential tails on FPU-like chains. Now, we want to demonstrate the main difference, namely the different time-dependence
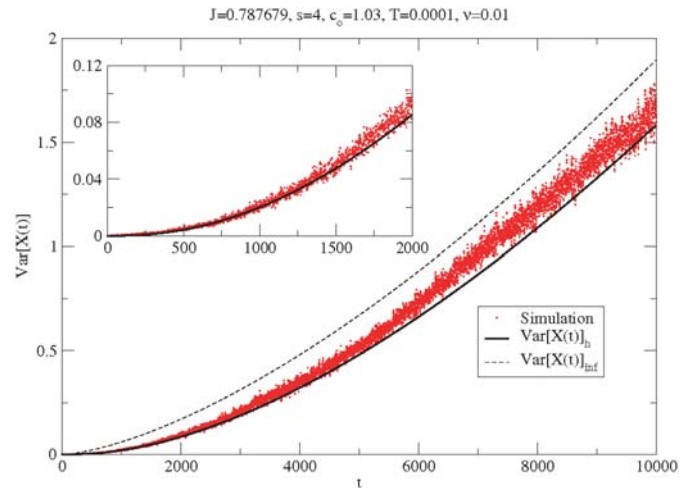

Fig. 3. (Color online) Position variance of a high-velocity soliton ($c_o = 1.03$) on an anharmonic chain with power-law long-range interactions ($J = 0.7877$, $s = 4$). The simulation and two different long-time approximations for (29), $\mathrm{Var}[X(t)]_{inf}$ (31) and $\mathrm{Var}[X(t)]_h$ (33), are shown. For $t = 10\,000$ ($t_r \approx 9$), the long-time limit is not yet reached, but the simulation results approach this function for long times.

of the superdiffusion in the two cases. We want to directly compare the results for $\mathrm{Var}[X(t)]$ and their time-dependence for two solitons with the same energy and velocity ($c_o = 1.03$) but one on a chain with power-law LRI and the other on a chain with Kac-Baker LRI. For the two solitons, normal diffusion contributions are negligible and the best fits in Figure 4 demonstrate that the position variance of algebraic solitons increases with $\sim t^{3/2}$ whereas for the *sech*-shaped solitons, the increase goes with a quadratic ($\sim t^2$) and a cubic ($\sim t^3$) term. The small-noise expansion results for both soliton types have the same long-time behaviour ($\sim t^{3/2}$) (compare with [23]) which is reached by the algebraic soliton in Figure 4 for $t > 8000$, whereas the exponential soliton is for times $t < 10\,000$ still in the regime where the long-time limit is not applicable. The Langevin systems for both soliton types are identical apart from the numerical constants and the values of the soliton parameters like the width. For Kac-Baker LRI, the inverse soliton width $\gamma_o = 0.132$ at $t = 0$ is distinctly smaller than for the power-law case with $\sigma_o = 0.279$ for the same energy and soliton velocity. Since the time scale t_r depends quadratically on the inverse width, it is not surprising that the long-time limit for exponential solitons is valid after much longer times. This argument is decisive for different solitons of the same type. It follows directly from the small-noise expansion that the long-time limit for the algebraic soliton with $c_o = 1.01$ appears for $\sigma_o^2(c_o = 1.03)/\sigma_o^2(c_o = 1.01) \approx 5.44$ longer times than for the algebraic soliton with $c_o = 1.03$.

In order to estimate when the exponential soliton reaches the long-time asymptotics, we have to concentrate our studies on the discussion of the result $\mathrm{Var}[X(t)]$ from the small-noise expansion for algebraic and exponential solitons (Fig. 5). Simulations for times much longer than
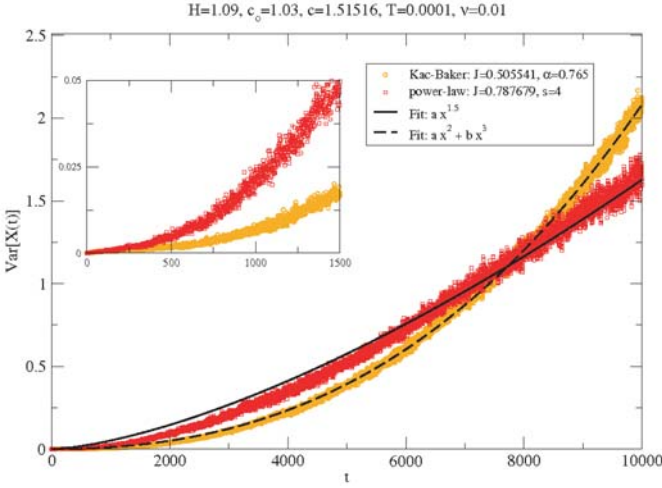
Fig. 4. (Color online) Simulation results for the position variance of two solitons, one on an anharmonic chain with power-law long-range interactions ($J = 0.7877$, $s = 4$) and the other soliton on an anharmonic chain with Kac-Baker long-range interactions for $T = 0.0001$. The interaction radius and the coupling for the Kac-Baker case were chosen in such a way that the two solitons have the same velocity $c_o = 1.03$ and the same energy. In order to demonstrate the difference in the time-dependence for the two solitons, we added a best fit for the two simulation results for Var$[X(t)]$. One can clearly see that the position variance of the algebraic soliton approaches a $\sim t^{1.5}$ time-dependence, whereas in the Kac-Baker case, the time-dependence can be fitted by a quadratic and a cubic term.

10^4 would be too time-consuming. The double-logarithmic scales in Figure 5 make clear that the Kac-Baker soliton reaches the long-time limit Var$[X(t)]_{inf}$ after much longer times than the power-law soliton. The time window where a stronger time-dependence than $\sim t^{3/2}$ appears is approximately ten times larger for the Kac-Baker soliton.

The influence of the soliton shape determines the diffusion constant in Var$[X(t)]_{inf}$, which is approximately a factor of π larger for exponential solitons. One can equivalently state that the longer transient times to the long-time limit for the exponential soliton is a consequence of the higher value of the diffusion constant. This remarkable difference for the two soliton types results only from the different soliton shapes because the numerical constant in (31) is determined by the numerical constants in the Langevin system (27) which follow from spatial integrations over the soliton profile in the CV procedure.

The time evolution of the velocity of the energetically equivalent algebraic and exponential soliton, $v_d(\sigma(t))$ and $v_d(\gamma(t))$, is rather different despite of the same start value and the structural similarities for v_d. In Figure 6, we present the simulation results for the mean velocity $\langle \dot{X}(t) \rangle$ of the two solitons in comparison with the zeroth order expressions for v_d from the small-noise expansion: $v_d(\sigma^{(0)}(t))$ and $v_d(\gamma^{(0)}(t))$ [23].

These hold for the zero temperature case but describe the mean velocity of the two noisy solitons already quite well. We can directly see that the power-law soliton ap-
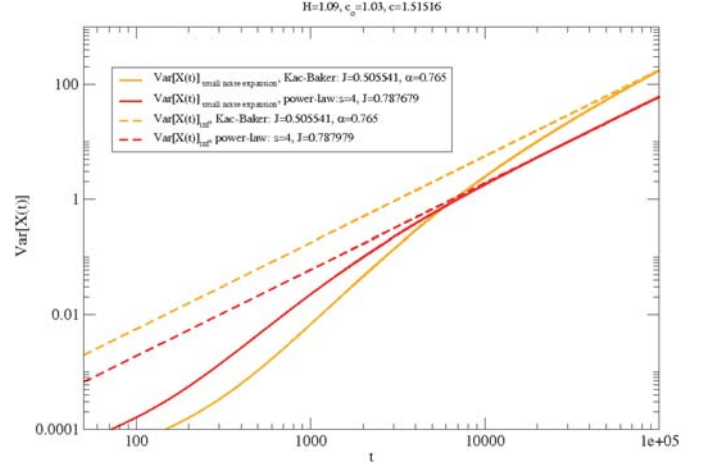

Fig. 5. (Color online) Var$[X(t)]$ and Var$[X(t)]_{inf}$ from a small-noise expansion for the two solitons of Figure 4. The algebraic soliton reaches the long-time limit Var$[X(t)]_{inf}$ much sooner than the exponential soliton with the same initial energy $H = 1.09$ and velocity $c_o = 1.03$. The result Var$[X(t)]_{inf}$ shows the same time-dependence but the diffusion constant for algebraic solitons is approximately a factor of π smaller.
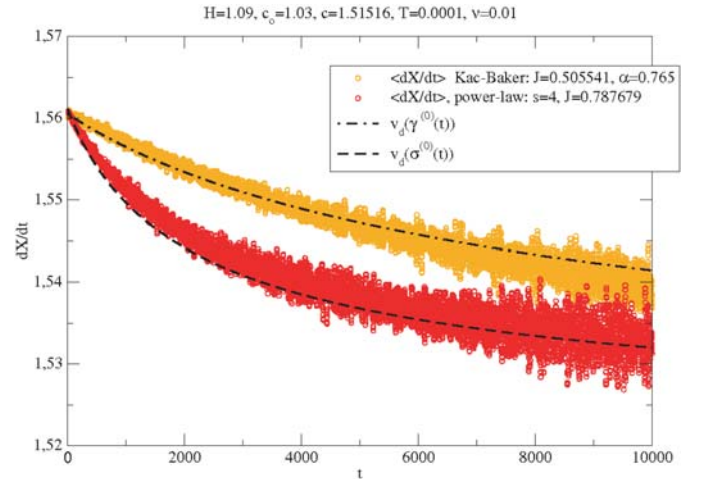

Fig. 6. (Color online) The simulation results for the mean soliton velocity $\langle \dot{X} \rangle$ in case of a noisy chain with $T = 0.0001$ for energetically equivalent algebraic and exponential solitons with $c_o = 1.03$. The zeroth-order results (without noise) for the soliton velocities $v_d(\sigma^{(0)}(t))$ and $v_d(\gamma^{(0)}(t))$ agree rather well with the simulation results and demonstrate the different dynamics of the two soliton types.

proaches the long-time limit with small soliton velocities earlier than the Kac-Baker soliton. The slower dynamics of the Kac-Baker soliton is caused by its broad, exponential shape and the resulting slower time scale t_r which controls the time-evolution of $\gamma^{(0)}(t)$. The dependence of v_d on a term $\sim \gamma^2$ for exponential solitons (which is negligible for algebraic solitons) influences the soliton velocity (and therefore the superdiffusion), especially for pronounced LRI character and for small times when the long-time limit is not yet reached.

8 Conclusions

We investigated the diffusion of algebraic solitons on FPU-like chains with power-law long-range interactions and derived analytically a result for the position variance which agrees well with the simulations of the discrete system. The results clearly reveal that the soliton diffusion and the damping-induced reshaping of the soliton depends on the time scale $t_r = \sigma_o^2 \nu_{hy} t$ which is given by the soliton width and the damping constant. For very broad solitons, the damping effects are quite weak because the particles in the soliton profile have moderate relative velocities and t_r evolves slowly in t. A small-noise expansion of the Langevin system yields an analytical result for the soliton diffusion which depends on t_r and predicts a superdiffusive long-time behaviour $\sim t^{3/2}$. This result makes clear why the superdiffusion, which sets in for large t_r, dominates the diffusion of high-energy solitons (σ_o^{-1} small). These basic features were also found in earlier studies for solitons with exponential shape. The superdiffusion of lattice solitons can therefore be regarded as generic when the lifetime of the solitons is much larger than $1/\sigma_o^2 \nu_{hy}$. On chains with NNI, this situation can often not be reached for low-energy solitons because they are rapidly destroyed by the fluctuations and the damping. *The LRI stabilize the soliton and lead to higher soliton energies and lifetimes which makes the superdiffusion the dominating mechanism.*

The shape of the soliton does not change the basics of the diffusion process. The Langevin systems for the collective variabels (inverse width and soliton position) are technically similar, only numerical constants and the dependence of the soliton velocity on the inverse width are different. We proved in simulations and by analyzing the analytical result that despite of the similarities, the superdiffusive behaviour of the two soliton types exhibits striking differences even when the soliton energy and velocity coincide. The algebraic solitons are generally narrower than exponential solitons which leads to faster dynamics for the time scale t_r and an earlier validity of the long-time limit with the characteristic $\sim t^{3/2}$ time-dependence. The broadness of the exponential solitons, the corresponding slower dynamics for t_r and the stronger dependence on higher orders of the inverse width in the soliton velocity shift the $\sim t^{3/2}$ region to larger times t which leads to the observed characteristic quadratic and cubic time-dependence in the simulations. *The perhaps most remarkable effect of the different soliton shapes is that the exponential solitons show larger position variances than their algebraic counterparts for sufficiently long times.* The diffusion constant in the long-time limit is for algebraic solitons approximately a factor of π smaller than for exponential solitons. This effect is only caused by the different soliton shapes which determine numerical constants in terms which describe the coupling between the soliton velocity and the fluctuations of the soliton width. Further studies for different values of s would be helpful to explain the influence of power-law interactions on the soliton diffusion. Especially the diffusion of solitons on chains with power-law LRI for the case $s < 3.5$ could be interesting because a gap between the plane-wave spectra and the soliton energies appears.

An important step would be analytical attempts to explain the simulations for superdiffusive high-amplitude localized modes as described in [25]. There, it was argued that scattering events are responsible for the superdiffusive behaviour. Surprisingly, the superdiffusive time-dependence $\sim t^{3/2}$ is exactly the same as in our studies for rather broad lattice solitons. However, in our case the superdiffusion mechanism is completely different.

Appndix A: Small-noise expansion

The small-noise expansion of the Langevin set (27) follows reference [34] and was already successfully applied to the problem of the diffusion of low-velocity solitons in the FPU system without long-range interactions [24]. We seek an asymptotic solution of the form

$$\sigma(t) = \sigma^{(0)}(t) + \epsilon \sigma^{(1)}(t) + ... \qquad (34)$$

$$X(t) = X^{(0)}(t) + \epsilon X^{(1)}(t) + ... \qquad (35)$$

where ϵ is a small parameter which is formally introduced to consider the influence of the noise terms as small perturbations ($\sqrt{D^{hy}} \sim \epsilon$). The contribution of the drift term in the different orders of ϵ are calculated following the rule

$$a_i(\sigma(t)) = a_i(\sigma^{(0)} + \sum_{m=1}^{\infty} \epsilon^m \sigma^{(m)}(t))$$

$$= a_i^{(0)}(t) + \epsilon \sigma^{(1)}(t) \frac{da_i(\sigma^{(0)}(t))}{d\sigma^{(0)}(t)} + ... \qquad (36)$$

In order to minimize the technical efforts, it is advisable to approximate the velocity $a_2 = v_d$ by the following expression

$$a_2 = \sqrt{c^2 + \frac{A_o}{2}\sigma(t) + \frac{\lambda}{2}\sigma^2(t)} \approx c\sqrt{1 + \frac{A_o}{2c^2}\sigma(t)}$$

$$\approx c + \frac{A_o}{4c}\sigma(t), \qquad (37)$$

which was checked to be appropriate for typical soliton parameters J, v. The equations in the order ϵ^0 read:

$$d\sigma^{(0)}(t) = -\frac{\nu_{hy}}{2}\sigma^{(0)}(t)^3 dt \qquad (38)$$

$$dX^{(0)}(t) = \left(c + \frac{A_0}{4c}\sigma(t)\right)dt. \qquad (39)$$

These equations describe the damped soliton. The damping induced broadening of the soliton is formally equivalent to the case of exponential soliton solutions in [23]. In the expression for the soliton velocity it is obvious that the damped soliton gets broader (smaller σ) which leads to a slowdown of the soliton. In the limit of long times, the soliton width diverges and the soliton approaches the velocity of sound.

The first order corrections due to the noise read:

$$d\sigma^{(1)}(t) = -\sigma^{(1)}(t)\frac{3}{2}\nu_{hy}(\sigma^{(0)}(t)^2)dt + \frac{\sqrt{D}\sigma^{(0)}(t)^{\frac{3}{2}}}{A_0\sqrt{\pi}v}dW_1$$

(40)

$$dX^{(1)}(t) = \sigma^{(1)}(t)\frac{A_0}{4c}dt + \frac{\sqrt{D}}{\sqrt{\sigma^{(0)}}\sqrt{\pi}A_0v}dW_2.$$

(41)

If we substitute the result for $\sigma^{(0)} = \sigma_o/\sqrt{\nu^{hy}\sigma_o^2t+1}$ into (41) we calculate the first-order expression for the dislocation of the soliton due to the noise

$$X^{(1)}(t) = \frac{\sqrt{D}\sigma_o^{(\frac{3}{2})}}{4c\sqrt{\pi}v}\int_0^t dt\eta'^{-\frac{3}{2}}\int_0^{t'}dt''\eta''^{\frac{3}{4}}dW_1(t'')$$

$$+\frac{\sqrt{D}}{\sigma_o\sqrt{\pi}A_ov}\int_0^t \eta'^{\frac{1}{4}}dW_2(t')$$

(42)

$$\eta' = 1 + \nu_{hy}\sigma_o^2t'.$$

(43)

After some straightforward calculations we can calculate the position varinace

$$\text{Var}[X^{(1)}(t)] = \lim_{s\to t}\langle X^{(1)}(t)X^{(1)}(s)\rangle.$$

(44)

References

1. A.C. Scott, *Nonlinear Science* (University Press Oxford, 1999)
2. *The Encyclopedia of Nonlinear Science*, edited by A.C. Scott (Routledge, New York, 2005)
3. T. Dauxois, M. Peyrard, *Physics of Solitons* (Cambridge University Press, 2005)
4. A.S. Davydov, *Solitons in Molecular Systems* (Reidel, Dotrecht, 1985)
5. A.C. Scott, Physics Reports **217**, 1 (1992)
6. M. Peyrard, Nonlinearity **17**, R1 (2004)
7. L.V. Yakushevich, J. Biosci. **26**, 305 (2001)
8. J. Edler, P. Hamm, A.C. Scott, Phys. Rev. Lett. **88**, 067403 (2002)
9. L. Cruzeiro-Hansson, S. Takeno, Phys. Rev. E, **56**, 894 (1997)
10. C.H. Choi, G. Kalosakas, K.Ø. Rasmussen, M. Hiromura, A.R. Bishop, A. Usheva, Nucleic Acids Res. **32**, 1584
11. Y.B. Gaididei, N. Flytzanis, A. Neuper, F.G. Mertens, Physica D **107**, 83
12. S. Flach, Phys. Rev. E **58**, R4116 (1998)
13. P.L. Christiansen, Y.B. Gaididei, F.G. Mertens, S.F. Mingaleev, Eur. Phys. J. B **19**, 545
14. S.F. Mingaleev, P.L. Christiansen, Yu.B. Gaididei, M. Johansson, K.Ø. Rasmussen, J. Biol. Phys. **25**, 41 (1999)
15. O.M. Braun, Yu. S. Kivshar, Physics Reports **306**, 1 (1998)
16. D. Bonart, Phys. Lett. A **231**, 201 (1997)
17. T. Rössler, J.B. Page, Phys. Rev. B **62**, 11460 (2000)
18. L. Cruzeiro-Hansson, Phys. Lett. A **249**, 465 (1998)
19. K.Ø. Rasmussen, P.L. Christiansen, M. Johansson, Yu. B. Gaididei, S.F. Mingaleev, Physica D **113**, 134 (1998)
20. *Dynamics and Thermodynamics of Systems with Long-Range Interactions*, edited by D. Ruffo, A. Wilkens Lecture Notes in Physics 602 (Springer, 2002)
21. C. Brunhuber, F.G. Mertens, Y. Gaididei, Phys. Rev. E **73**, 016614 (2006)
22. S.F. Mingaleev, Y.B. Gaididei, F.G. Mertens, Phys. Rev. E **61**, R1044
23. C. Brunhuber, F.G. Mertens, Y. Gaididei, Phys. Rev. E **75**, 036615 (2007)
24. E. Arévalo, F.G. Mertens, Y. Gaididei, A.R. Bishop, Phys. Rev. E **67**, 016610 (2003)
25. R. Reigada, A. Sarmiento, K. Lindenberg, Phys. Rev. E **64**, 066608 (2001)
26. S. Mingaleev, Y. Gaididei, F.G. Mertens, Phys. Rev. E **58**, 3833 (1998)
27. A.S. Cârstea, D. Grecu, Anca Vişinescu, Phys. Lett. A, **246**, 82 (1998)
28. Y. Ishimori, Prog. Theor. Phys. **68**, 402 (1982)
29. E. Arévalo, F.G. Mertens, A.R. Bishop, Eur. Phys. J. B **27** 63 (2002)
30. L.A. Ostrovsky, E.N. Pelinovsky, Sov. Phys. Dokl. **15**, 1097 (1971)
31. A. Jeffrey, T. Kawahara, *Asymptotic Methods in Nonlinear Wave Theory* (Pitman, London, 1982)
32. C. Brunhuber, F.G. Mertens, Y. Gaididei, Eur. Phys. J. B **42**, 103 (2004)
33. V. Konotop, L. Vázquez, *Nonlinear Random Waves* (World Scientific, Singapore, 1994)
34. C.W. Gardiner, *Handbook of Stochastic Methods* (Springer-Verlag, New York-Heidelberg-Berlin, 1983)
35. F.G. Mertens, E. Arévalo, A.R. Bishop, Phys. Rev. E **72**, 036617 (2005)
36. E. Arévalo, Dissertation (Universität Bayreuth, 2004)